Impeded inverse energy transfer in the Charney–Hasegawa–Mima model of quasi-geostrophic flows

By CHUONG V. TRAN AND DAVID G. DRITSCHEL

School of Mathematics and Statistics, University of St Andrews, St Andrews KY16 9SS, UK

The behaviour of turbulent flows within the single-layer quasi-geostrophic (Charney–Hasegawa–Mima) model is shown to be strongly dependent on the Rossby deformation wavenumber λ (or free-surface elasticity). Herein, we derive a bound on the inverse energy transfer, specifically on the growth rate $d\ell/dt$ of the characteristic length scale ℓ representing the energy centroid. It is found that $d\ell/dt \leqslant 2\|q\|_\infty/(\ell_s\lambda^2)$, where $\|q\|_\infty$ is the supremum of the potential vorticity and ℓ_s represents the potential enstrophy centroid of the reservoir, both invariant. This result implies that in the potential-energy-dominated regime ($\ell \geqslant \ell_s \gg \lambda^{-1}$), the inverse energy transfer is strongly impeded, in the sense that under the usual time scale no significant transfer of energy to larger scales occurs. The physical implication is that the elasticity of the free surface impedes turbulent energy transfer in wavenumber space, effectively rendering large-scale vortices long-lived and inactive. Results from numerical simulations of forced-dissipative turbulence confirm this prediction.

1. Introduction

The atmosphere and oceans are greatly influenced by the background planetary rotation and stable density stratification. These features almost suppress motion in the vertical direction, rendering geophysical fluid systems, intrinsically vast in their horizontal extent compared with their limited depth, approximately two-dimensional at large scales. Many models derived from the theory of quasi-geostrophy exploit this simplification. One such model, governed by the Charney–Hasegawa–Mima (CHM) equation, is the subject of the present study.

The CHM equation, which describes the evolution of potential vorticity in a shallow fluid layer with a free-surface, takes the form (Pedlosky 1987)

$$\frac{\partial q}{\partial t} + J(\psi, q) = 0. \tag{1.1}$$

Here $\psi(x, y, t)$, the streamfunction, is assumed to be periodic in both x and y. Note that ψ is proportional to the free-surface height anomaly. The quantity $q = (\Delta - \lambda^2)\psi$ is the potential vorticity, where λ is the Rossby deformation wavenumber ($\lambda = f/c$, where f is the Coriolis frequency and c is the small-scale gravity wave speed, both assumed constant). (Note that this form of potential vorticity ignores the so-called β-term. For some studies concerning the effects of this term, see Kukhakin & Orszag (1996), Okunu & Masuda (2003) and Smith (2004).) The differential operators $J(\cdot, \cdot)$ and Δ are, respectively, the Jacobian and two-dimensional Laplacian.

Equation (1.1) expresses material conservation of potential vorticity. It also governs the evolution of quasi-two-dimensional fluctuations of the electrostatic potential in a plane perpendicular to a strong magnetic field applied uniformly to a plasma, in which case ψ is the electrostatic potential and λ^{-1} is the ion Larmor radius (Hasegawa & Mima 1978).

The CHM equation has been a subject of active research for decades (see for example, Hasegawa & Mima 1978; Fyfe & Montgomery 1979; Yanase & Yamada 1984; Larichev & McWilliams 1991; Ottaviani & Krommes 1992; Kukharkin, Orszag & Yakhot 1995; Iwayama, Shepherd & Watanabe 2002; Arbic & Flierl 2003; Tran & Bowman 2003). A majority of these studies have been concerned with the dual transfer of the total energy $\langle -\psi q \rangle/2 = \langle |\nabla\psi|^2 \rangle/2 + \lambda^2 \langle \psi^2 \rangle/2$ and potential enstrophy $\langle \Delta\psi q \rangle/2 = \langle |\Delta\psi|^2 \rangle/2 + \lambda^2 \langle |\nabla\psi|^2 \rangle/2$, which are conserved by the CHM nonlinearities. Here $\langle \cdot \rangle$ denotes a spatial average. The kinetic energy and the usual enstrophy are $\langle |\nabla\psi|^2 \rangle/2$ and $\langle |\Delta\psi|^2 \rangle/2$, respectively (these are not conserved). The quantity $\lambda^2 \langle \psi^2 \rangle/2$ is the potential energy. In addition to the total energy and potential enstrophy, the CHM dynamics also conserve an infinite class of potential vorticity norms, including the L^∞ norm $\|q\|_\infty$. Similar to two-dimensional Navier–Stokes (NS) turbulence, the dual conservation law implies that the total energy (potential enstrophy) is preferentially transferred to lower (higher) wavenumbers. Unlike two-dimensional NS turbulence, each of the invariants in CHM turbulence consists of two components. The presence of the second component is due to the elasticity of the free surface, which is known to have a fundamental influence on the dynamics. A remarkable effect is that the inverse energy transfer for wavenumbers $k \ll \lambda$ (the so-called potential energy regime) is predominantly a transfer of the potential energy (Tran & Bowman 2003), i.e. of the quadratic quantity $\langle \psi^2 \rangle$. For scales smaller than $\lambda^{-1} = c/f$, the motion is inherently three-dimensional (cf. Dritschel & de la Torre Juárez 1996; Dritschel, de la Torre Juárez & Ambaum 1999) and therefore poorly described by (1.1).

Numerical studies of CHM turbulence appear to suggest that in the potential energy regime, the inverse cascade is strongly impeded. For turbulence decaying from an initial energy reservoir, Larichev & McWilliams (1991) observe a 'slowness' in the turbulent evolution. Iwayama *et al.* (2002) notice the formation of a sharp spectral peak, a manifestation of an inverse energy transfer with limited extent in wavenumber space. Arbic & Flierl (2003) find that the inverse cascade slows down and that vortex merging takes a very long time. For forced turbulence, Kukharkin *et al.* (1995) observe the formation of vortical 'quasicrystals', states of long-lived inactive vortices. While these observations are consistent with the finding of Tran & Bowman (2003) that the inverse energy transfer involves virtually no kinetic energy when $k \ll \lambda$, they are not fully explained by this fact. A more satisfactory explanation would be that the inverse transfer of potential energy is also impeded in this regime.

In this note we derive an upper bound for the growth rate of a characteristic length scale associated with the inverse energy transfer. We infer from this upper bound that in the potential energy regime, the inverse energy transfer is strongly impeded by the elasticity of the free surface. An interesting physical interpretation of this effect is that this elasticity prohibits the merger of large-scale vortices to form larger energy-carrying scales, effectively rendering such vortices long-lived and inactive. Although this effect is deduced in the framework of unforced and inviscid dynamics, it also manifests itself in a forced-dissipative version of (1.1), as is illustrated by some numerical results.

2. Inverse energy transfer

The nonlinear transfer of energy to lower wavenumbers of an energy reservoir (when it occurs) necessarily entails an increase of a suitably defined length scale representing the energy centroid of the reservoir. Here we consider the length scale ℓ defined by

$$\ell = \frac{\langle(-\Delta)^{-1/2}\psi q\rangle}{\langle\psi q\rangle} = \frac{\langle|(-\Delta)^{1/4}\psi|^2\rangle + \lambda^2\langle|(-\Delta)^{-1/4}\psi|^2\rangle}{\langle|\nabla\psi|^2\rangle + \lambda^2\langle\psi^2\rangle}. \tag{2.1}$$

In (2.1) the operator $(-\Delta)^\theta$ is defined by $(-\Delta)^\theta\widehat{\psi}(\boldsymbol{k}) = k^{2\theta}\widehat{\psi}(\boldsymbol{k})$, where $k = |\boldsymbol{k}|$ is the wavenumber and $\widehat{\psi}(\boldsymbol{k})$ the Fourier transform of $\psi(\boldsymbol{x})$. The growth rate $\mathrm{d}\ell/\mathrm{d}t$ provides a quantitative measure of the inverse transfer. In particular, a smaller rate corresponds to an inverse transfer with a more limited extent in wavenumber space than one with a greater rate. In this respect, $\mathrm{d}\ell/\mathrm{d}t$ may be considered as a measure of locality of the inverse transfer, in the sense that for a given energy distribution a smaller rate implies a more local transfer than a greater one.

In the case where most of the kinetic energy resides in wavenumbers $k \ll \lambda$ (the potential energy regime), $\langle|(-\Delta)^{1/4}\psi|^2\rangle$ is negligible compared with $\lambda^2\langle|(-\Delta)^{-1/4}\psi|^2\rangle$, and similarly $\langle|\nabla\psi|^2\rangle$ is negligible compared with $\lambda^2\langle\psi^2\rangle$. More precisely, in this regime we have

$$\frac{\langle|(-\Delta)^{1/4}\psi|^2\rangle}{\lambda^2\langle|(-\Delta)^{-1/4}\psi|^2\rangle} \leqslant \frac{\langle|\nabla\psi|^2\rangle}{\lambda^2\langle\psi^2\rangle} \ll 1,$$

where the first inequality is due to Hölder's inequality (see also Tran & Shepherd 2002 and Tran 2004), implying $\ell \approx \langle|(-\Delta)^{-1/4}\psi|^2\rangle/\langle\psi^2\rangle$. For an energy reservoir in the potential energy regime, the length scale ℓ specifies where, in wavenumber space, most of $\langle\psi^2\rangle$ (or equivalently most of the potential energy) is distributed. Its growth rate is thus the rate at which the spectral profile of the potential energy proceeds toward lower wavenumbers.

The evolution equation for the characteristic length scale ℓ, defined in the preceding paragraphs, is obtained by multiplying (1.1) by $(-\Delta)^{-1/2}\psi/\langle\psi q\rangle$ and taking the spatial average of the resulting equation:

$$\begin{aligned}
\frac{1}{2}\frac{\mathrm{d}\ell}{\mathrm{d}t} &= \frac{\langle(-\Delta)^{-1/2}\psi J(\psi, q)\rangle}{\langle|\nabla\psi|^2\rangle + \lambda^2\langle\psi^2\rangle} = -\frac{\langle q J(\psi, (-\Delta)^{-1/2}\psi)\rangle}{\langle|\nabla\psi|^2\rangle + \lambda^2\langle\psi^2\rangle} \\
&\leqslant \frac{\langle|q||\nabla\psi||\nabla(-\Delta)^{-1/2}\psi|\rangle}{\langle|\nabla\psi|^2\rangle + \lambda^2\langle\psi^2\rangle} \leqslant \frac{\langle|\nabla\psi|^2\rangle^{1/2}\langle\psi^2\rangle^{1/2}}{\langle|\nabla\psi|^2\rangle + \lambda^2\langle\psi^2\rangle}\|q\|_\infty,
\end{aligned} \tag{2.2}$$

where the various manipulations of the nonlinear term are straightforward. In particular, the last step can be readily seen by expressing the streamfunction in terms of a Fourier series.

The ratio in front of $\|q\|_\infty$ on the right-hand side of (2.2) can be closely estimated in terms of conserved quantities. For that purpose, let us denote by ℓ_s the conserved length scale representing the enstrophy centroid of the reservoir:

$$\ell_s = \frac{\langle-\psi q\rangle^{1/2}}{\langle\Delta\psi q\rangle^{1/2}} = \frac{(\langle|\nabla\psi|^2\rangle + \lambda^2\langle\psi^2\rangle)^{1/2}}{(\langle|\Delta\psi|^2\rangle + \lambda^2\langle|\nabla\psi|^2\rangle)^{1/2}}. \tag{2.3}$$

Solving (2.3) for $\langle\psi^2\rangle$ and substituting the result into the said ratio we obtain

$$
\begin{aligned}
\frac{\langle|\nabla\psi|^2\rangle^{1/2}\langle\psi^2\rangle^{1/2}}{\langle|\nabla\psi|^2\rangle + \lambda^2\langle\psi^2\rangle} &= \frac{\langle|\nabla\psi|^2\rangle^{1/2}\left[\ell_s^2\langle|\Delta\psi|^2\rangle + (\ell_s^2\lambda^2 - 1)\langle|\nabla\psi|^2\rangle\right]^{1/2}}{\lambda\left[\langle|\nabla\psi|^2\rangle + \ell_s^2\langle|\Delta\psi|^2\rangle + (\ell_s^2\lambda^2 - 1)\langle|\nabla\psi|^2\rangle\right]} \\
&\leqslant \frac{\langle|\nabla\psi|^2\rangle^{1/2}(\langle|\Delta\psi|^2\rangle + \lambda^2\langle|\nabla\psi|^2\rangle)^{1/2}}{\ell_s\lambda(\langle|\Delta\psi|^2\rangle + \lambda^2\langle|\nabla\psi|^2\rangle)} \\
&= \frac{\langle|\nabla\psi|^2\rangle^{1/2}}{\ell_s\lambda(\langle|\Delta\psi|^2\rangle + \lambda^2\langle|\nabla\psi|^2\rangle)^{1/2}} \leqslant \frac{1}{\ell_s\lambda^2}.
\end{aligned}
\tag{2.4}
$$

This is a very sharp estimate, especially for a reservoir in the potential energy regime. We note that in general the inequality $\ell \geqslant \ell_s$ holds. This is a consequence of the Hölder inequality and can be shown as follows. Let us denote by $U(k)$ the power spectrum of $\langle-(-\Delta)^{-1/2}\psi q\rangle$. The length sales ℓ and ℓ_s can then be expressed in terms of $U(k)$ as

$$
\ell = \frac{\displaystyle\int U(k)\,\mathrm{d}k}{\displaystyle\int kU(k)\,\mathrm{d}k}
$$

and

$$
\ell_s = \left(\frac{\displaystyle\int kU(k)\,\mathrm{d}k}{\displaystyle\int k^3U(k)\,\mathrm{d}k}\right)^{1/2}.
$$

Now by Hölder's inequality we have

$$
\int kU(k)\,\mathrm{d}k \leqslant \left(\int U(k)\,\mathrm{d}k\right)^{2/3}\left(\int k^3U(k)\,\mathrm{d}k\right)^{1/3},
$$

from which the inequality $\ell \geqslant \ell_s$ indeed follows immediately.

Putting these results together we have

$$
\frac{\mathrm{d}\ell}{\mathrm{d}t} \leqslant 2\frac{\|q\|_\infty}{\ell_s\lambda^2} \leqslant 2\frac{\|q\|_\infty}{\ell_s^2\lambda^2}\ell
\tag{2.5}
$$

where we have used $\ell \geqslant \ell_s$. Hence the exponential growth rate of ℓ is bounded from above by $2\|q\|_\infty/(\ell_s^2\lambda^2)$. Given a finite $\|q\|_\infty$, the upper bound $2\|q\|_\infty/(\ell_s^2\lambda^2)$ can be made arbitrarily small provided $\ell_s^2\lambda^2$ is sufficiently large. This condition is satisfied for an initial energy reservoir in a sufficiently remote wavenumber region of the potential energy regime, where both $\ell_s\lambda \gg 1$ and $\ell\lambda \gg 1$. Under these circumstances, no significant growth of ℓ occurs when the initial energy reservoir freely spreads out, and hence no significant inverse energy transfer is possible. In passing it is worth mentioning that the upper bound for the exponential growth rate of ℓ in (2.5) consists of the constant λ and the two invariants $\|q\|_\infty$ and ℓ_s, and therefore can be completely determined by initial data.

The result in the preceding paragraph is an analytic version of the qualitative statement in the literature that the turbulence evolves on a rescaled (slower) time (cf. Larichev & McWilliams 1991; Kukharkin *et al.* 1995). To clarify this point let us rewrite (2.5) as

$$\ell_s^2 \lambda^2 \frac{\mathrm{d}\ell}{\mathrm{d}t} \leqslant 2\|q\|_\infty \ell. \tag{2.6}$$

The left-hand side of (2.6) is the (instantaneous) growth rate of ℓ on the slow time $\tau = t/(\ell_s^2 \lambda^2)$. For an initial reservoir with a finite $\|q\|_\infty$, the inverse transfer of potential energy can be considerable only on this slow time scale. In the limit $\ell_s \lambda \to \infty$, the invariants become $\langle \psi^2 \rangle/2$ and $\langle |\nabla \psi|^2 \rangle/2$ and the length scales ℓ and ℓ_s become $\langle |(-\Delta)^{-1/4} \psi|^2 \rangle / \langle \psi^2 \rangle$ and $\langle \psi^2 \rangle^{1/2} / \langle |\nabla \psi|^2 \rangle^{1/2}$, respectively. The rescaled time τ becomes infinitely long.

An estimate which may be significantly sharper than (2.5) can be derived by replacing the potential vorticity q in (2.2) by the relative vorticity $\Delta \psi$. By doing that, instead of (2.5), we obtain

$$\frac{\mathrm{d}\ell}{\mathrm{d}t} \leqslant 2 \frac{\|\Delta \psi\|_\infty}{\ell_s^2 \lambda^2} \ell. \tag{2.7}$$

In remote regions of the potential energy regime, where $\ell \lambda \geqslant \ell_s \lambda \gg 1$, we expect $\lambda^2 \psi$ to dominate $\Delta \psi$. Therefore in these regions it is plausible that $\|q\|_\infty \gg \|\Delta \psi\|_\infty$, allowing (2.7) to become significantly sharper than (2.5). The price for this improvement is that $\|\Delta \psi\|_\infty$ is not conserved. Note that in such regions ℓ and ℓ_s are the length scales of potential and kinetic energy, respectively.

A straightforward physical interpretation of the above result is that the elasticity of the free surface suppresses energy transfer for scales larger than the Rossby deformation radius. This effect has a profound influence on the vortex dynamics. Let us consider a hypothetical flow consisting of vortices (having smooth potential vorticity – no small length scales) of comparable scales, which are much larger than the deformation radius λ^{-1}. For these scales the inverse energy transfer is strongly impeded, allowing virtually no formation of larger energy-carrying scales. This keeps the vortices from merging, effectively establishing a state of long-lived inactive vortices. This may explain the crystallization of vortices observed by Kukharkin *et al.* (1995). The impeded inverse energy transfer implies a similar effect on the direct transfer of potential enstrophy, a consequence of the dual conservation law. One can see from the 'symmetry' of the dual conservation law that the available potential enstrophy for direct transfer depends on the inversely transferred energy. Similarly, the available energy for inverse transfer depends on the directly transferred potential enstrophy. Hence impeded inverse energy transfer means impeded direct potential enstrophy transfer (and vice versa). This implies that smooth potential vorticity with scales $\gg \lambda^{-1}$ remains smooth.

3. Numerical results

We now consider results obtained from numerical simulations of a forced-dissipative version of (1.1). These convincingly illustrate the strong reduction of the inverse transfer in the potential energy regime, and may help explain an observation by Iwayama *et al.* (2002) in their numerical simulations of freely decaying CHM turbulence wherein an initial energy reservoir evolves into a single sharp peak. A plausible explanation for this observation is that the sharp peak is due to both the viscous dissipation (which suppresses the formation of small scales) and the impeded inverse transfer deduced in the preceding section: their collective effect 'squeezes' energy into a narrow band of wavenumbers, resulting in the observed peak. In our forced-dissipative case we observe that in the potential energy regime the inverse
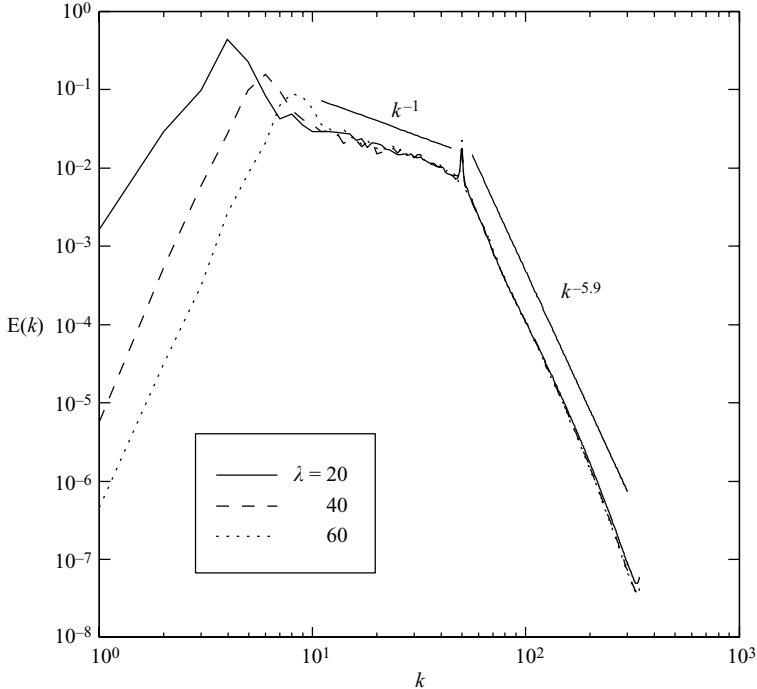
FIGURE 1. The kinetic energy spectrum $E(k)$ vs. k averaged over periods [139, 140], [155, 156] and [160, 161] for $\lambda = 20$, 40 and 60, respectively.

energy flux is arrested and deposits most of the potential energy at the lower-wavenumber end of the quasi-steady energy range. We also observe a relaxation of the kinetic energy spectrum of the inertial range (from $k^{-5/3}$ toward k^{-1}) as the inverse cascade proceeds from $k > \lambda$ to $k < \lambda$.

We simulate (1.1), with the addition of molecular viscosity and a body force, in a doubly periodic square $2\pi \times 2\pi$ with a dealiased 1024^2 pseudospectral method. No large-scale dissipation mechanisms are employed and no steady dynamics are sought since we are primarily interested in the near arrest of the inverse energy cascade in a quasi-steady state. (For an analysis of steady CHM turbulence in the presence of large-scale damping, see Smith *et al.* 2002.) Three different values of λ are used: $\lambda = 20, 40$ and 60. The forcing is spectrally localized in the wavenumber interval $K = [49.5, 50.5]$, in the sense that its Fourier components $\widehat{f}(\boldsymbol{k})$ are non-zero only for those modes $\boldsymbol{k}$ having magnitudes k lying in the interval K:

$$\widehat{f}(\boldsymbol{k}) = \frac{\epsilon}{N} \frac{\widehat{\psi}(\boldsymbol{k})}{\sum_{|\boldsymbol{p}|=k} |\widehat{\psi}(\boldsymbol{p})|^2}. \tag{3.1}$$

Here $\epsilon = 1$ is the constant energy injection rate and N is the number of distinct wavenumbers in K. The viscosity coefficient is $\nu = 5 \times 10^{-4}$. The simulations were initialized with the kinetic energy spectrum $E(k) = 10^{-5}\pi k/(50^2 + k^2)$.

Figure 1 shows the quasi-steady kinetic energy spectrum $E(k)$ vs. k averaged over periods [139, 140], [155, 156] and [160, 161] for $\lambda = 20, 40$ and 60, respectively. In all three cases, the accumulation of energy at low wavenumbers is clearly visible.
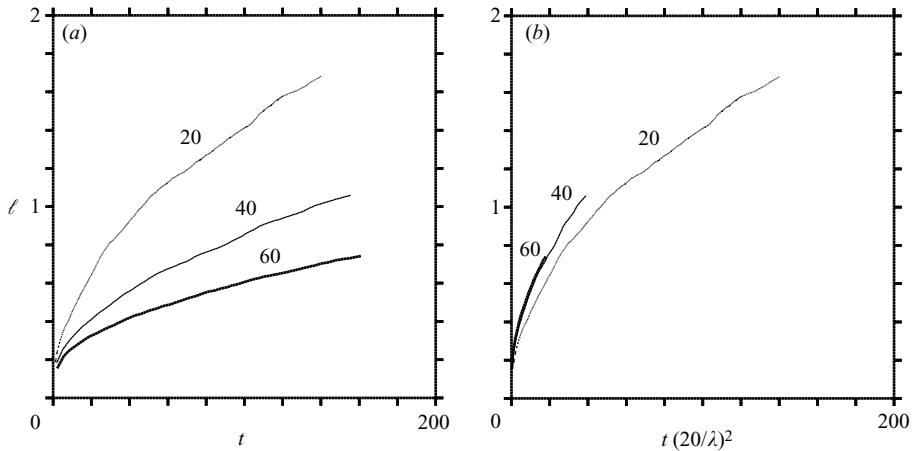
FIGURE 2. The energy centroid ℓ versus time t (a) and scaled time $t(20/\lambda)^2$ (b) for $\lambda = 20$, 40 and 60, as labelled.

This is attributed to the impeding effect discussed above, and not finite-size effects since the energy levels at the lowest wavenumbers are still small compared with the energy peaks. This is true for both kinetic and potential components. For $\lambda = 20$ we have a limited kinetic energy regime in the wavenumber interval [20, 50]. Before the energy peak reaches $\lambda = 20$, the dynamics of this kinetic energy regime are expected to resemble those of two-dimensional NS turbulence: the energy cascades to low wavenumbers via a $k^{-5/3}$ kinetic energy spectrum. We indeed observe a discernible $k^{-5/3}$ spectrum (not shown) in the wavenumber range [20, 50] before the energy peak reaches $\lambda = 20$. The dynamics after the energy peak passes λ undergo profound changes. Most notably, the growth of potential energy occurs mainly around the energy peak, consistent with the reduction of the inverse energy transfer in the conservative case. Another remarkable change is in the spectral slope of the energy spectrum from $k = \lambda = 20$ up to the forcing wavenumber $k = 50$. The slope of the kinetic energy spectrum in this region appears to relax from $-5/3$ to -1. The quasi-steady† spectrum becomes k^{-1} with an excessive accumulation of energy at the lower-wavenumber end. This unexpected feature is common to the other two cases, for which hardly any inverse transfer region exists between the forcing wavenumber and λ and for which no clear $k^{-5/3}$ spectrum is formed initially.

The evolution of the energy centroid ℓ for these three cases is shown in figure 2(a) versus unscaled time t and in figure 2(b) versus scaled time $t(20/\lambda)^2$. Both the reduction in $d\ell/dt$ with increasing λ and the collapse of the curves when plotted versus scaled time are consistent with the growth rate bound (2.5). (Note, however that we cannot directly compare the numerical growth rates with the theoretical bound because the imposed forcing violates conservation of $\|q\|_\infty$ and ℓ_s used in (2.5).) Only the $\lambda = 20$ case stands out slightly, due to an early kinetic energy transfer which is virtually absent in the other two cases.

† Note that after the energy peak passes λ, growth of energy is due primarily to that of the potential energy and the kinetic energy becomes quasi-steady.

4. Summary and discussion

The main result of this work is an upper bound for the growth rate of the characteristic length scale associated with the inverse energy transfer in CHM turbulence. This upper bound is expressible in terms of the supremum of the potential vorticity, the characteristic length scale representing the potential enstrophy centroid of the reservoir and the Rossby deformation radius. These are constants of motion, allowing the bound to be completely described in terms of initial data. It is found that in remote regions of the potential energy regime, the turbulent transfer from an initial energy reservoir becomes strongly impeded, in the sense that hardly any potential energy is transferred to lower wavenumbers. This effect has been illustrated by numerical simulations of a forced-dissipative version of the CHM equation. The physical implication of the present finding is that the elasticity of the free surface hinders the nonlinear transfer of potential energy to larger scales.

An interesting implication of the present result is that vortices having smooth potential vorticity and scales much larger than the Rossby deformation radius are kept from merging to form larger energy-carrying scales and remain smooth. Such vortices are inactive and long-lived compared to their counterparts in two-dimensional NS turbulence.

The present theory is fully consistent with other results for both forced (Kukharkin *et al.* 1995) and freely decaying (Larichev & McWilliams 1991; Iwayama *et al.* 2002; Arbic & Flierl 2003) CHM turbulence, as discussed above. These, we argue, are explained by the growth rate bound (2.6) and its physical interpretations given at the end of §2.

Analyses of atmospheric and oceanic data yield results that could plausibly be explained by the present work. Boer & Shepherd (1983) find that the spectral flux in atmospheric wind data is arrested with essentially no inertial range. Scott & Wang (2005) find the inverse energy transfer in the oceans to be qualitatively similar to the result of Boer & Shepherd (1983). These are in remarkable agreement with the idealized numerical results noted above and with the present findings.

Iwayama *et al.* (2002) observe 'well-behaved' tails of the potential vorticity probability density function (PDF) – much steeper than observed in NS turbulence, see their figure 5 – and raise the question of why it is that CHM turbulence in the potential energy regime exhibits no intermittency. A speculative answer provided by the authors is based on an asymptotic version of the CHM equation wherein the relative vorticity is dropped from the time-derivative term:

$$\lambda^2 \frac{\partial \psi}{\partial t} + J(\Delta \psi, \psi) = 0.$$

This equation, as noted by Iwayama *et al.* (2002), describes advection of ψ by $\Delta \psi$ (i.e. by the smaller scales of motion). These authors argue that this may lead to more 'random walk' behaviour, effectively suppressing intermittency. The present study provides an alternative answer: the reduction of turbulent transfer both renders large-scale vortices inactive and discourages erratic small-scale motion. This also can account for the observed steep PDF. In some sense CHM turbulence in the potential energy regime is far less turbulent than its two-dimensional NS counterpart.

REFERENCES

ARBIC, B. K. & FLIERL, G. R. 2003 Coherent vortices and kinetic energy ribbons in asymptotic, quasi two-dimensional f-plane turbulence. *Phys. Fluids* **15**, 2177–2189.

BOER, G. J. & SHEPHERD, T. G. 1983 Large-scale two-dimensional turbulence in the atmosphere. *J. Atmos. Sci.* **40**, 164–184.

DRITSCHEL, D. G. & DE LA TORRE JUÁREZ, M. 1996 The instability and breakdown of tall columnar vortices in a quasi-geostrophic fluid. *J. Fluid Mech.* **328**, 129–160.

DRITSCHEL, D. G., DE LA TORRE JUÁREZ, M. & AMBAUM, M. H. P. 1999 The three dimensional vortical nature of atmospheric and oceanic turbulent flows. *Phys. Fluids* **11**, 1512–1520.

FYFE, D. & MONTGOMERY, D. 1979 Possible inverse cascade behaviour for drift-wave turbulence. *Phys. Fluids* **22**, 246–248.

HASEGAWA, A. & MIMA, K. 1978 Pseudo-three-dimensional turbulence in magnetized nonuniform plasma. *Phys. Fluids* **21**, 87–92.

IWAYAMA, T., SHEPHERD, T. G. & WATANABE, T. 2002 An 'ideal' form of decaying two-dimensional turbulence. *J. Fluid Mech.* **456**, 183–198.

KUKHARKIN, N. & ORSZAG, S. A. 1996 Generation and structure of Rossby vortices in rotating fluids. *Phys. Rev. E* **54**, 4524–4527.

KUKHARKIN, N., ORSZAG, S. A. & YAKHOT, V. 1995 Quasicrystallization of vortices in drift-wave turbulence. *Phys. Rev. Lett.* **75**, 2486–2489.

LARICHEV, V. D. & MCWILLIAMS, J. C. 1991 Weakly decaying turbulence in an equivalent-barotropic fluid. *Phys. Fluids* A **3**, 938–950.

OKUNO, A. & MASUDA, A. 2003 Effects of horizontal divergence on the geostrophic turbulence on a beta-plane: suppression of the Rhines effect. *Phys. Fluids* **15**, 56–65.

OTTAVIANI, M. & KROMMES, J. A. 1992 Weak- and strong-turbulence regimes of the forced Hasegawa–Mima equation. *Phys. Rev. Lett.* **69**, 2923–2026.

PEDLOSKY, J. 1987 *Geophysical Fluid Dynamics,* 2nd Edn. Springer.

SCOTT, R. B. & WANG, F. 2005 Direct evidence of an oceanic inverse kinetic energy cascade from satellite altimetry. *J. Phys. Oceanogr.* **35**, 1650–1666.

SMITH, K. S. 2004 A local model for planetary atmospheres forced by small-scale convection. *J. Atmos. Sci.* **61**, 1420–1433.

SMITH, K. S., BOCCALETTI, G., HENNING, C. C., MARINOV, I. N., TAM, C. Y., HELD, I. M. & VALLIS, G. K. 2002 Turbulence diffusion in the geostrophic inverse cascade. *J. Fluid Mech.* **469**, 13–48.

TRAN, C. V. 2004 Nonlinear transfer and spectral distribution of energy in α turbulence. *Physica* D **191**, 137–155.

TRAN, C. V. & BOWMAN, J. C. 2003 Energy budgets in Charney–Hasegawa–Mima and surface quasigeostrophic turbulence. *Phys. Rev. E* **68**, 036304.

TRAN, C. V. & SHEPHERD, T. G. 2002 Constraints on the spectral distribution of energy and enstrophy dissipation in forced two-dimensional turbulence. *Physica* D **165**, 199–212.

YANASE, S. & YAMADA, M. 1984 The effect of the finite Rossby radius on two-dimensional isotropic turbulence. *J. Phys. Soc. Japan* **53**, 2513–2520.